Six Phase Permanent Magnet Machine with Fractional Slot Concentrated Winding

Rudolf Krall
University of Leoben
Austria, Leoben 8700
Email: rudolf.krall@unileoben.ac.at

Johann Krenn
University of Leoben
Austria, Leoben 8700
Email: johann.krenn@unileoben.ac.at

Helmut Weiss
University of Leoben
Austria, Leoben 8700
Email: helmut.weiss@unileoben.ac.at

***Abstract*—Permanent Magnet Machines (PMM) with a phase number (*m*) higher than three allow redundancy and lower torque ripple compared to their three phase counterparts.**
In this paper, a six phase permanent magnet machine with surface rotor magnets, designed with fractional slot tooth winding is proposed. A stator design with fractional slot tooth winding allows the design of a compact machine through shorter end winding and less copper volume. Fractional slot tooth windings cause additional space harmonics in the air gap which cause additional torque ripple and rotor losses (iron and magnet losses). The influence of the tooth winding (with single layer and double layer layout) and the influence of the higher number of phases on the torque ripple of a sinusoidal fed PM-machine are discussed. The paper includes winding design consideration for single and double layer winding layout. Criteria for feasible slot/pole combinations for the two winding variants are proposed. An analytical way to calculate the Magneto motive force (*MMF*), counting for the space harmonics in the air gap, is illustrated. With the *MMF* distribution in the air gap, the average torque and the current related torque ripple for the *PMM* with surface rotor magnets is calculated analytical. The analytically results are compared with a Finite element (*FEM*) calculation.

Keywords*—*Multiphase, fractional slot winding, single layer, double layer, winding function, MMF distribution, torque ripple

I. Introduction

Multiphase machines, with a phase number (*m*) higher than three, exhibit less torque ripple and higher fault tolerance. This paper will deal with a six phase Permanent Magnet Machine with surface rotor magnets (*PMM*), designed with a short pitched fractional slot winding, which is also called tooth winding. In such a winding configuration, the number of slots per phase and per pole (*q*) is not an integer. A machine design with a tooth winding allows having a compact machine due to smaller end windings. The copper volume of the machine can be reduced by using this winding design technique. A detailed description of advantages, opportunities and challenges for machines with fractional slot winding can be found in [1].The winding layout can be done in single layer (*SL*) and double layer (*DL*) architecture. In the *DL* layout, each slot contains two coil sides which are laying side by side. In the *SL* architecture, each slot occupies only one coil side (*see Fig.1*).This paper deals with design considerations and criteria for the selection of the optimum slot pole combination. This will be done for different number of phases and for *SL* and *DL* design respectively.

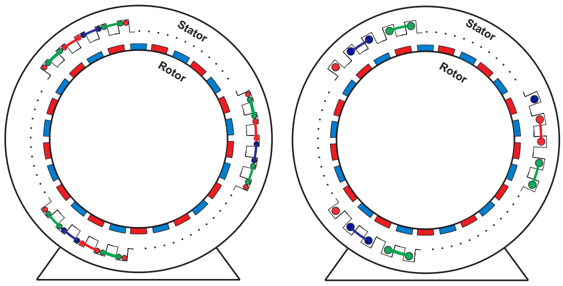

Fig. 1. Basic Scheme of a SL and DL Stator winding

Beside the torque producing magnetomotive force (*MMF*) component (fundamental or synchronous component) in the air gap, fractional slot windings generate a wide spectrum of space harmonics. The orders of these harmonics are above and could be below the fundamental order as well. These harmonics cause additional torque ripple and rotor losses.

II. Design Considerations

For a certain number of phases only some slot pole combinations are feasible. Tab.I shows possible slot/pole pair (*p*) combinations for different number of phases. The investigation covers phase numbers (*m*) of 3, 4, 5, 6, 7 and 9 and $q < 1$. By selecting a slot pole combination, the possible phase numbers for a *DL* or *SL* design can be found by Tab.I. The subscript '*' denotes that the design can be realized for *SL* architecture as well. The number of slots are shortened by N_s.
In order to design the machine with a symmetrical winding, the nominator q_z and denominator q_n of q must not have a $gcd > 1$ (*greatest common divisor*). If q_n and the phase number *m* have a $gcd > 1$, a tooth winding design is not possible as well [2].

$$q = \frac{N_s}{2p \cdot m} = \frac{q_z}{q_n} \tag{1}$$

$$gcd(q_z, q_n) = 1 \text{ and } gcd(q_n, m) = 1 \tag{2}$$

A *DL* layout is feasible if (3) is fullfilled.

$$\frac{2p}{q_n} \in integer \tag{3}$$

For a *SL* configuration and an odd number of phases, the quantity of stator slots must be at least twice the number of phases. For a multiphase configuration with an even number of phases, the quantity of stator slots must be at least four times of *m*.

$$\frac{N_s}{2 \cdot m} \in integer, \text{ for m is odd} \tag{4}$$

$$\frac{N_s}{4 \cdot m} \in integer, \text{ for m is even} \tag{5}$$

For the electrical constraints, the periodicity of the machine is significant.

$$t_p = gcd(N_s, p) \tag{6}$$

If t_p is greater than one, there are t_p electrically equal slot sequences containing $N_s' = N_s/t_p$ slots in the armature. The feasibility for constructing a single layer winding must be done by (4) and (5) and by using N_s' instead of N_s. If N_s'/m is an even number, N_s' slots span a base winding of first grade in which the number of poles-pairs per base winding p' is equal to p/t_p. If N_s'/m is an odd number, N_s' slots span a base winding of second grade for a double layer winding were $p' = p/t_p$. A base winding of the second grade, constructed as a single layer winding requires $2N_s'$ slots. In this case, the number of pole-pairs is equal to $p' = 2p/t_p$. Due to the interaction of the rotor magnets with the stator slots, a torque ripple is produced. This additional torque ripple is called cogging torque. The number of cogging torque periods per full mechanical rotation is determined by the lowest common multiple (*lcm*) of N_s and the number of poles (*2p*) [3], [4]. Tab.II indicates the *lcm* for the pole slot combinations which allow the design of a fractional slot winding according to Tab.I. By choosing the highest $lcm(N_s, 2p)$, the cogging torque behavior can be improved.

TABLE I. SLOT POLE COMBINATIONS FOR DIFFERENT NUMBER OF PHASES

p	N_s	3	6	9	12	15	18	21	24
1		3		9					
2		3	3*	3,9		5	9*	7	
3				3		5		7	
4		3	3*	3,9	3*	3,5	3*,9*	3,7	
5		3	3*	3,9	3*,6	3	3*,9*	3,7	3*,4,6*
6				3		5	3	7	
7		3	3*	3,9	3*,6	3,5	3*,9*	3	3*,4,6*
8		3	3*	3,9	3*	3,5	3*,9*	3,7	3*
9						5		7	4
10		3	3*	3,9	3*	3	3*,9*	3,7	3*,6
11		3	3*	3,9	3*,6	3,5	3*,9*	3,7	3*,4,6*
12				3		5	3*	7	

TABLE II. LCM OF NUMBER OF SLOTS(N_s) AND NUMBER OF POLEPAIRS (P)

p	N_s	3	6	9	12	15	18	21	24
1		6	6	18					
2		12	12	36		60	36	84	
3				18		30		42	
4		24	24	72	24	120	72	168	
5		30	30	90	60	30	90	210	120
6				36		60	36	84	
7		42	42	126	84	210	126	42	168
8		48	48	144	48	240	144	336	48
9						90		126	72
10		60	60	180	60	60	180	420	120
11		66	66	198	132	330	198	462	264
12				72		120	72	168	

The winding configuration for *SL* and *DL* is done based on the star of slots.

Guidelines for using the star of slots and rules for selecting phasors are described in [2], [5], [6] and [7].

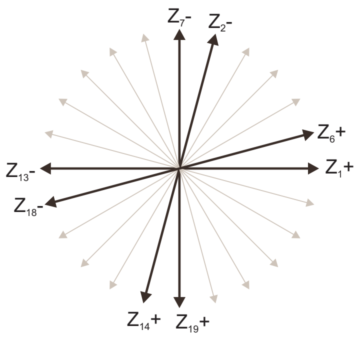

Fig. 2. Star of slots for the fundamental component

TABLE III. WINDING FACTOR FOR SIX PHASE MACHINE

p	N_s	12	24	
5		0.966	0.604	DL
		-	**0.604**	**SL**
7		0.966	0.604	DL
		-	**0.604**	**SL**
11		0.259	0.983	DL
		-	**0.991**	**SL**

III. WINDING FACTOR

The winding factor ζ_w for the main harmonic component (main space harmonic) is proportional to the electromagnetic torque generation and should be as high as possible. Designs with low fundamental winding factors require higher number of turns and higher currents, respectively, for same power. This will lead to higher copper losses, if the design should be for the same torque, slot fill factor and magnetic loading.

A high fundamental winding factor can be obtained if $2p \approx N_s$ [4].The winding factor determination for individual harmonics can be done with the star of slots. A geometrical sum of all phasors belonging to one phase and a further scaling by the the linear sum of the absolute phasor values, leads to the winding factor. Important to note is, that phasors referring to negative coil sides must be considered negative. The phasors in Fig.2, denote with $'+'$ or $'-'$ exponent, are referring to the positive and negative coil sides respectively. Assuming that the star of slots in Fig.2 is drawn for the main harmonic (fundamental) component and the bold drawn phasors belonging to a particular phase, the winding factor ζ_w can calculated by using equation (7).

$$\zeta_w(\nu) = \frac{\left|\sum_i \underline{Z}_i^+(\nu) - \sum_k \underline{Z}_k^-(\nu)\right|}{\sum_i \left|\underline{Z}_i^+(\nu)\right| + \sum_k \left|\underline{Z}_k^-(\nu)\right|} \tag{7}$$

Equation (7) shows the mathematical expression for calculating ζ_w, were ν indicates the harmonic order.

Tab.III shows the winding factor for the main harmonic component, identified for a six phase machine with different slot/pole combinations (*SL,DL*). The slot factor, which is part of the winding factor, is not considered if the star of slots is used to determine the winding factor.

IV. ANALYTICAL MMF CALCULATION

The MMF calculation is based on the winding function of a single coil. Important to note is, that the following elaborations are done for a periodicity of one base winding. Fig.3 shows the winding function of one coil over a period of 2π with respect to a base winding period. The corresponding fourier series for an arbitrary coil of a phase winding is shown in (8). Fig.3 shows also the difference in the winding function behavior in the slot open area between a double layer and a single layer layout.

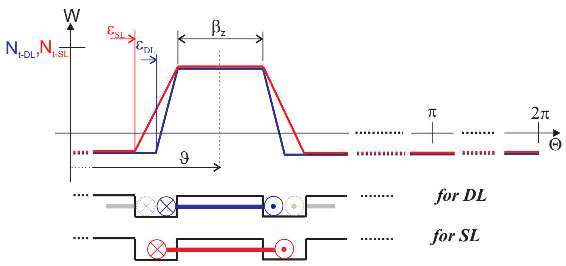

Fig. 3. Winding function of 1 coil over a period of 2π

$$\underline{W}(\theta) = \frac{2N_t}{\pi} \cdot \sum_k \frac{1}{k} \cdot \underbrace{\sin\left(\frac{\beta_z + \varepsilon}{2} k\right)}_{\zeta_S(k)} \cdot \underbrace{\frac{\sin(\varepsilon k/2)}{\varepsilon k/2}}_{\zeta_N(k)} \cdot e^{i(k\theta - k\vartheta)} \tag{8}$$

$$k = 1, 2, 3, \ldots, \infty$$

The variable N_t defines the number of turns per coil, β_z is the tooth angle, ε is the slot open angle and ϑ_x considers the position of the coil on the circumference within 2π of a base winding. In case of $t_p = 1$, β_z and ε are equal to the mechanical dimension. Otherwise the mechanical values must be multiplied by the periodicity t_p. The factors $\zeta_S(k)$ and $\zeta_N(k)$ are introduced as pitch factor and slot factor respectively. The MMF produced by one coil, fed by a sinusoidal current I_x with a angular frequency ω, is defined as follows:

$$\underline{F}_x(\theta, t) = \underline{W}_x(\theta) \cdot \Re\{I_x \cdot e^{i(\omega t - \phi_x)}\} \tag{9}$$

Fractional slot winding designs for an even phase number are always base windings of the first grade. Therefore, the further deviation for the total MMF is done only for a base winding of the first grade which are characterized by an odd numbered denominator q_n. If q_n is odd, each slot has an opposite slot, belonging to the same phase which carries the same current with reverse polarity. The winding functions of one phase within a periodicity of a base winding is the sum of the winding function of each coil. In case of a base winding of the first grade and if $q_z = 1$, the final form of the fourier expression of the winding function for one phase is shown in (10).

$$\underline{W}_x(\theta) = \frac{4N_t}{\pi} \cdot \sum_h \frac{1}{h} \cdot \zeta_S(h) \cdot \zeta_N(h) \cdot e^{i(h\theta - h\vartheta_x)} \tag{10}$$

$$h = 1, 3, 5, \ldots, \infty$$

The total MMF within the periodicity of one base winding follows the relation in (11).

$$\underline{F}(\theta, t) = \sum_{x=1}^{m} \underline{W}_x(\theta) \cdot \Re\{I_x \cdot e^{i(\omega t - \phi_x)}\} \tag{11}$$

The design of a fractional slot winding requires, that the phases are spatially shifted by $\frac{\pi}{m}$ related to the main harmonic component, which has the order p'. As mentioned above, p' is the number of pole pairs for a base winding. The phase currents are time shifted by $\frac{\pi}{m}$, as usual. For the further analytical deviation of the total MMF, it is assumed that the coils are spatially shifted by $\frac{\pi}{m}$ related to the first order space harmonic but the phase currents are shifted in time by $\frac{p'\pi}{m}$. This step is physically correct and generates the same MMF distribution over the circumference. Equation (11) can be re-written into equation (12).

$$\begin{aligned}\underline{F}(\theta, t) =& \frac{4N_t}{\pi} \cdot \sum_h \zeta_S(h) \cdot \zeta_N(h) \cdot \frac{1}{h} \sum_{j=1}^{m} e^{i\left(h\theta - \frac{\pi}{m}h(j-1)\right)} \\ &\cdot \frac{I}{2} \left[e^{i\left(\omega t - \frac{\pi}{m}hp'(j-1)\right)} + e^{-i\left(\omega t - \frac{\pi}{m}hp'(j-1)\right)} \right]\end{aligned} \tag{12}$$

By progressing the integer j from 1 to the number of phase m, the term in the brace of (12) results in:

$$\ldots \frac{I}{2} \cdot e^{i(\omega t + h\theta)} \underbrace{\left\{ 1 + e^{-i\left(\frac{\pi}{m}(h+p')\right)} + \ldots + e^{-i\left(\frac{(m-1)\pi}{m}(h+p')\right)} \right\}}_{\neq 0 \text{ if } (h+p'=2mY)} +$$

$$+ \frac{I}{2} \cdot e^{i(\omega t - h\theta)} \underbrace{\left\{ 1 + e^{-i\left(\frac{\pi}{m}(h-p')\right)} + \ldots + e^{-i\left(\frac{(m-1)\pi}{m}(h-p')\right)} \right\}}_{\neq 0 \text{ if } (h-p'=2mY)}$$

$$Y = 0, 1, 2, 3, \ldots, \infty$$

The total MMF distribution over a circumference of a base winding exhibits space harmonics of the order $n = p' \pm 2mY$. The fourier series of the total MMF according to equation (12) can be simplified into equation (13).

$$\underline{F}(\theta, t) = m \cdot \frac{2N_t I}{\pi} \cdot \sum_n \zeta_S(n) \cdot \zeta_N(n) \cdot \frac{1}{n} \cdot e^{i(\omega t - n\theta)} \tag{13}$$

V. Torque Calculation

The torque is calculated based on the Maxwell Stress Tensor theory [8]. The total torque exerted on the rotor can be obtained by integrating the stress tensor for instance over a cylinder that confines the rotor. The torque is defined according to (14), were r is the radius and l is the axial length of the cylinder. The parameters $B_n(\theta, t)$ and $H_t(\theta, t)$ determine the radial component of the magnetic flux density and the tangential magnetic field strength respectively. Both occur on the surface of the rotor confining cylinder.

$$T(t) = r^2 l \int_0^{2\pi} B_n(\theta, t) \cdot H_t(\theta, t) d\theta \tag{14}$$

For further torque calculation, we assume that the flux density of the magnets has only a radial component and iron saturation and slotting effects are neglected. Using the Ampères law, the tangential magnetic field strength $H_t(\theta, t)$ on the surface of the stator bore is equal to the linear current density $A(t, \theta)$.

$$\underline{H}_t(\theta, t) = \underline{A}(\theta, t)$$

The linear current density is deviated from the MMF distribution, following (15).

$$\begin{aligned}\underline{A}(\theta, t) =& \frac{1}{r} \frac{d\underline{F}(\theta, t)}{d\theta} \\ =& -i \frac{m}{r} \frac{2N_t I}{\pi} \sum_n \zeta_S(n) \cdot \zeta_N(n) \cdot e^{i(\omega t - n\theta)}\end{aligned} \tag{15}$$

The fourier series of the radial field in the air gap, coming from the rotor over a period of a base winding is defined according to (16) and shown in Fig.4. The mechanical speed is considered by ω_m and δ_0 can be used to define an initial rotor position.The rotor pole width is defined by β_B which is the mechanical pole width angle multiplied by the number of pole pairs. The amplitude of the magnetic flux density is defined by $\hat{B}_n$.

$$\underline{B}_n(\theta,t) = \frac{4\hat{B}_n}{\pi}\cdot\sum_z \zeta_B(z)\frac{1}{z}e^{i\left(z\omega_m p' t - z(p'\theta-\delta_0)\right)} \quad (16)$$
$$\zeta_B(z) = \sin\left(\frac{\beta_B}{2}z\right)$$
$$z = 1,3,5,\ldots,\infty$$

The torque over the surface of the rotor confining cylinder can

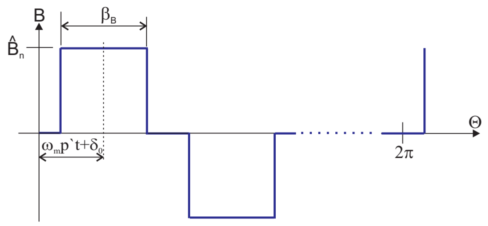

Fig. 4. Magnetic flux density in radial direction

be calculated by using (15) and (16) in (14) where $H_t(\theta,t) = \Re(\underline{H}_t(\theta,t))$ and $B_n(\theta,t) = \Re(\underline{B}_n(\theta,t))$.

$$\begin{aligned} T(t) =& rl\frac{8N_t\hat{B}_n Im}{2\pi^2}\cdot\sum_z\sum_n \zeta_S(n)\zeta_N(n)\zeta_B(z)\frac{1}{z}\cdot \\ &\cdot\left\{\int_0^{2\pi}\sin\left((\omega t - z\omega_m t p') - \theta(n-zp') - z\delta_0\right)d\theta + \right. \\ &\left. + \int_0^{2\pi}\sin\left((\omega t + z\omega_m t p') - \theta(n+zp') + z\delta_0\right)d\theta\right\} \end{aligned} \quad (17)$$

An average torque over 2π only occurs if $z\cdot p'$ has the same order than n. Considering this aspect, equation (17) can be simplified in equation (18), were $\nu = p' \pm 2p'mY$ defines the space harmonic orders which will cause an average torque over 2π. The variable Y is kept as $0,1,2,3,\ldots,\infty$.

$$\begin{aligned} T(t) = rl\frac{8N_t\hat{B}_n Imp'}{\pi}\cdot\sum_\nu \zeta_S(\nu)\zeta_N(\nu)\zeta_B(\frac{\nu}{p'})\frac{1}{\nu}\cdot \\ \cdot\sin\left((\omega-\omega_m\nu)t - \frac{\nu}{p'}\delta_0\right) \end{aligned} \quad (18)$$

The previous deviation of the torque is only valid for a base winding of the first grade and a numerator q_z which is equal to 1. If q_z is greater than one, the torque equation (18) will follow in equation (19), were $q'_z = q_z$ for DL design and $q'_z = q_z/2$ for a SL design. ζ_Z is introduced as belt factor and ζ_W represents the winding factor. In addition, it is assumed that the mechanical speed is equal to the synchr. speed $(\omega_m = \omega/p')$.

$$\begin{aligned} T(t) =& rl\frac{8N_t\hat{B}_n Imp'q'_z}{\pi}\cdot\sum_\nu \underbrace{\zeta_S(\nu)\zeta_N(\nu)\zeta_Z(\nu)}_{\zeta_W(\nu)}\zeta_B(\frac{\nu}{p'})\cdot \\ &\cdot\frac{1}{\nu}\sin\left((1-\frac{\nu}{p'})\omega t - \frac{\nu}{p'}(\delta_0-\phi_{\zeta Z})\right) \end{aligned} \quad (19)$$
$$\zeta_Z(\nu) = \frac{\sin\left(q'_z\nu\alpha_z/2p'\right)}{q'_z\sin\left(\nu\alpha_z/2p'\right)}$$
$$\phi_{\zeta Z} = \frac{(q'_z-1)\alpha_z}{2}$$
$$\alpha_z = \frac{2\pi}{N'_s}\text{ (for DL) or } \alpha_z = 2\frac{2\pi}{N'_s}\text{ (for SL)}$$

By averaging (19) over one cycle, the steady state torque produced by the machine will result. This torque is constant with respect to time. Constant torque over time can only be generated by the main space harmonic component of ν which requires that $\nu = p'$.

$$\begin{aligned} \overline{T} =& \frac{1}{\tau_p}\int_0^t T(t)dt \\ =& rl\frac{8N_t\hat{B}_n Imp'q'_z}{\pi}\zeta_W(p')\zeta_B(1)\sin(\phi_{\zeta Z}-\delta_0) \end{aligned} \quad (20)$$

The term $(\phi_{\zeta Z} - \delta_0)$ defines the phase angle between the main harmonic component of the MMF and the main harmonic component of the rotor radial magnetic flux density. To gain maximum torque, this angle difference should be $\pm\pi/2$. The total torque of the machine in case of $t_p > 1$ is shown in (21).

$$T_{tot}(t) = t_p\cdot T(t) \quad \overline{T}_{tot} = t_p\cdot\overline{T} \quad (21)$$

The orders of the space harmonics over the whole circumference of the machine are $\nu_{tot} = t_p\cdot\nu$. The spectrum of the time harmonics in the machine torque are independent of t_p.

VI. Analytical vs. Numerical Calculation

In the following section the electromagnetic torque in the air gap is calculated according to the analytical torque equations and numerically by FEM software, for a particular machine. The FEM simulation was done without considering saturation effects of the stator iron. The torque calculation was done for a six phase, 10 pole and 12 slots machine with a double layer tooth winding layout. The rotor is designed with surface mounted magnets. More detailed machine parameters are listed in Tab.IV.

TABLE IV. Machine data

number of phases	6	
Phase current	14	A
number of turns per coil	108	
frequency	50	Hz
remanenz flux density	1.2	T
rotor pole width	30.6	°
number of stator slots	12	
number of rotor poles	10	
stator bore radius	100.5	mm
magnet hight	4.9	mm
mech. air gap length	1.3	mm
slot width	26.3	mm
tooth width	26.3	mm
slot depth	25	mm
iron length	135	mm

Fig.5 shows the total MMF distribution over 2π. The MMF distribution is done at $t = 0s$. The plot faces the analytical

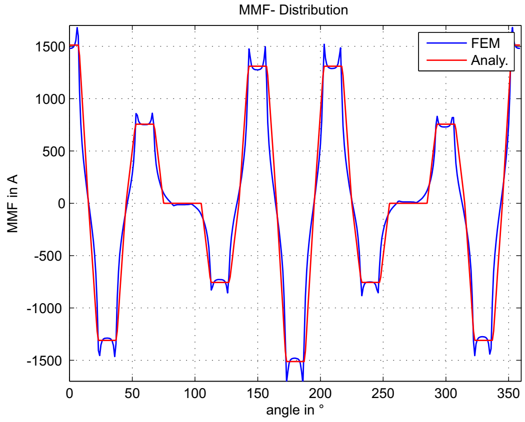

Fig. 5. MMF distribution over 2π

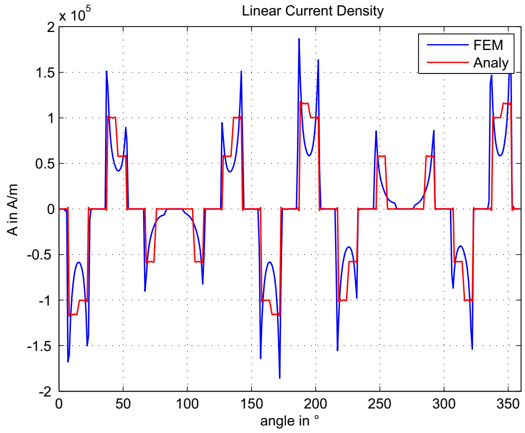

Fig. 6. Linear current density distribution over 2π

result versus the numerical from the FEM software. On the border between slot and tooth, the numerical solution shows high peaks in the MMF result. A possible explanation could be inherent numerical problems at these corner points.

Fig.6 shows the MMF related current density distribution at the same time. Neglecting the peaks at the beginning and the end of each slot, the numerical result fits with the analytical solution, especially if we consider some averaging. Fig.7 shows the electromagnetic torque trend over $6ms$ while the supply frequency was $50Hz$. The torque calculation was done with open slots. Open slots are a standard for a machine with tooth winding design. The slot opening decrease the flux density in the slot area. This effect is considered by reducing the amplitude of the magnetic flux density by selecting a carter factor of 0.75 for the analytical calculation. The mean value over the time period are fitting quite well. The dominant space harmonic of the order $\nu = -55$, which results in a 12^{th} time harmonic, is visible in both results. The influence of the $\nu = -115$ and $\nu = 125$, which results in a 24^{th} and 25^{th} time harmonics, are not visible in the numerical solution any more. The current related torque ripple is around 1.3% of the rated torque.

VII. Conclusion

Fractional slot windings in tooth coil technology allow designing compact machines because of shorter end winding.

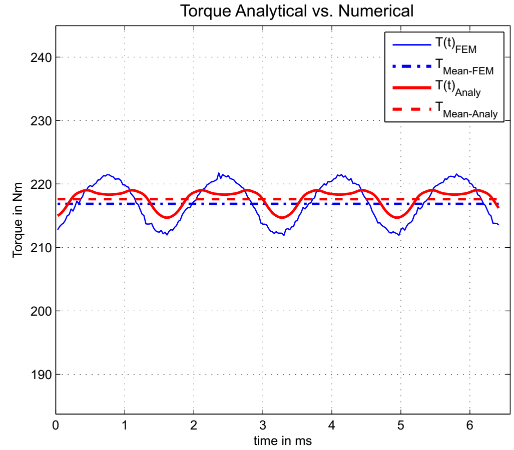

Fig. 7. Torque trend over a time period of 6ms

This winding technique can be used for a single layer and double layer winding layout. A drawback of the tooth winding technology is the wide spectrum of MMF harmonics. Therefore, the current related torque ripple will increase. Multiphase machines allow a reduction of the current related torque ripple. The paper proposes design rules for machines with tooth coil technology for an arbitrary phase number. The aim of the paper was to propose an analytical way to calculate the torque of the machine with fraction slot winding of the first grade, which takes into account all space harmonics. The analytical results showed good conformity to the numerical ones.

References

[1] A. EL-Refaie, "Fractional-slot concentrated-windings synchronous permanent magnet machines: Opportunities and challenges," *Industrial Electronics, IEEE Transactions on*, vol. 57, no. 1, pp. 107–121, 2010.

[2] K. Vogt, *Berechnung elektrischer Maschinen*. VCH Verlag, 1996, no. 3-527-28391-9.

[3] A. EL-Refaie, "High speed operation of permanent magnet machines," Ph.D. dissertation, University of Wisconsin Madison, 2005.

[4] G. Huth, "Permanent-magnet-excited ac servo motors in tooth-coil technology," *Energy Conversion, IEEE Transactions on*, vol. 20, no. 2, pp. 300–307, 2005.

[5] H. Jussila, P. Salminen, M. Niemela, and J. Pyrhonen, "Guidelines for designing concentrated winding fractional slot permanent magnet machines," in *Power Engineering, Energy and Electrical Drives, 2007. POWERENG 2007. International Conference on*, 2007, pp. 191–194.

[6] E. Fornasiero, L. Alberti, N. Bianchi, and S. Bolognani, "Considerations on selecting fractional-slot nonoverlapped coil windings," *Industry Applications, IEEE Transactions on*, vol. 49, no. 3, pp. 1316–1324, 2013.

[7] N. Bianchi and M. Dai Pre, "Use of the star of slots in designing fractional-slot single-layer synchronous motors," *Electric Power Applications, IEE Proceedings* -, vol. 153, no. 3, pp. 459–466, 2006.

[8] G. Mueller, *Theorie elektrischer Maschinen*. VCH Verlag, 1995, no. 3-527-28392-7.